Bull. Chem. Soc. Ethiop. **2024**, 38(4), 1129-1144.
DOI: https://dx.doi.org/10.4314/bcse.v38i4.25

ISSN 1011-3924
Printed in Ethiopia
Online ISSN 1726-801X

SYNTHESIS OF NEW PEPTIDE-BASED MACROCYCLES: EVALUATION OF THEIR IN VITRO ANTI-PROLIFERATIVE ACTIVITY AND MOLECULAR DYNAMIC SIMULATION STUDIES

Gaber O. Moustafa[1*], Abdulrahman A. Almehizia[2], Mohamed A. Al-Omar[2], Abdulrahman M. Al-Obaid[2], Ahmed M. Naglah[2] and Amer A. Zen[3]

[1]Peptide Chemistry Department, Chemical Industries Research Institution, National Research Centre, 12622-Dokki, Cairo, Egypt
[2]Department of Pharmaceutical Chemistry, College of Pharmacy, King Saud University, P.O. Box 2457, Riyadh 11451, Saudi Arabia
[3]Chemistry & Forensics Department, Clifton Campus, Nottingham Trent University, Nottingham Ng11 8NS, UK

(Received February 16, 2024; Revised April 8, 2024; Accepted April 10, 2024)

ABSTRACT. A simplified synthetic protocol was adopted for the preparation of the six novel cyclo-pentapeptide candidates of the structure cyclo-(*m*-phthaloyl)-*bis*-[*L*-Phe -Gly/Sar]-*L*-Lys–X, where X = COOMe (**9a**,**b**), COOH (**10a**,**b**) and $NHNH_2$ (**11a**,**b**). The potential cytotoxicity (IC_{50}, µg/mL) for cyclo-pentapeptides **(9a**,**b)**, **(10a**,**b)**, **(11a**,**b)** and doxorubicin® as reference drugs, is assayed against eight cell lines of human cancer namely; mamillary *MCF-7* and *T47D*, hepatic *HEPG2*, colon *HCT116*, cell line of cervix *HELA*, larynx *HEP2*, Prostate *PC3*, and gut *Caco*. Cyclo-[*m*-phthaloyl chloride-*bis*-(*L*-phalanine-sar)-*L*-Lys]-COOH **10b** was proved as cytotoxically more potent than doxorubicin against most of the screened cell lines. It can be inferred that the proposed molecular structural characteristics associated with cytotoxicity in these *m*-phthaloyl-bridged cyclopeptides appear noteworthy and hold promise as potential candidates for further exploration as novel anticancer agents. Molecular dynamics simulation studies of **10b** into the binding site of Human Epidermal Growth Factor Receptor tyrosine kinase exhibited the highest MM-GBSA value (-16.59 kcal/mol).

KEY WORDS: Anticancer, Cytotoxicity, Cyclopeptides, *m*-phthaloyl-bis-peptides

INTRODUCTION

Considering the increased universal mortality rates, as well as the accompanying health and socio-economical drawbacks, the search for potent anticancer medications with superior chemo therapeutic index and minimized side effects reflects true scientific challenges [1-5]. It is worth noting that it has been mentioned in many references that natural and synthetic peptides have very distinctive biological activity in all different applied directions [6-15]. In this context, peptides are considered less potent drugs primarily because of their low bioavailability, even though they present convenient initial synthetic drug prototypes that are relatively easy to assemble in terms of structure and modulate pharmacologically. Therefore, synthesized proteins, serving as preliminary biological leads, enable the swift determination of molecular structural features associated with more potent drug principles. Consequently, an increasing number of both natural and synthetic peptides with noteworthy biological activities are being reported [16-18].

In essence, molecular cyclization introduces traditional conformational constraints, leading to lower entropy levels. As a result, cyclopeptides generally exhibit enhanced pharmacological characteristics compared to their linear counterparts. This increased stability against proteolytic enzymes contributes to prolonged bioavailability [19-21]. This accounts for the finding that drug development and synthetic drug discovery or natural anticancer cyclopeptides become,

*Corresponding authors. E-mail: gosman79@gmail.com

particularly, a promising approach [22-25]. As typical examples of anticancer cyclopeptides, the "FDA" approved natural bicyclic cyclo-peptide Romidepsin (Istodax®) (**I**) is used for the treatment of peripheral T-cell lymphoma, which is a cancer of a type of white blood cells called T-cells, which are part of the immune system [26] (Figure 1).

Moreover, the well-known drug "*Actinomycine D* is an inhibitor of RNA synthesis and acts as a potent inducer of apoptosis in several cell lines" such as PANC-1 pancreatic cancer cells [27] (Figure 1). In addition, *m*-picolonyl bridged cyclo-pentapeptide (**III**) (Figure 1) was reported as a potent anticancer agent against mamillary cancer cell line NCF7 and central nervous system cancer cell line SF-268 [24].

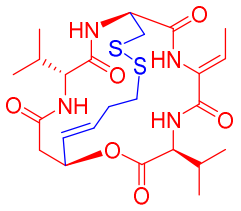

Cyclo-pentapeptides
Istodax Romidepsin (FK228) (I)

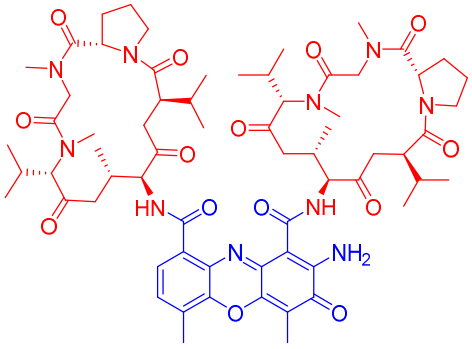

Bi-cyclo-pentapeptides
Actinomycin D (Dactinomycin) (II)

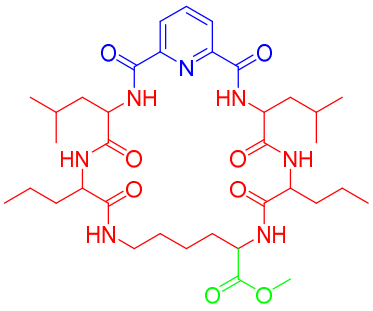

Cyclo-(dipicolinoyl)-pentapeptide **(III)**

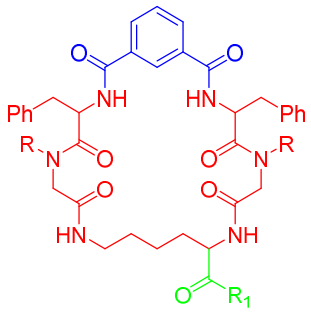

9-11

9a, R = H, R_1 = OMe
9b, R = Me, R_1 = OMe
10a, R = H, R_1 = OH
10b, R = Me, R_1 = OH
11a, R = H, R_1 = $NHNH_2$
11b, R = Me, R_1 = $NHNH_2$

Figure 1. Structure of anticancer agents cyclo-pentapeptides istodax romidepsin (FK228) (**I**), actinomycin D (dactinomycin) (**II**), cyclo-(picolinoyl)-pentapeptide (**III**), the targeted cyclo-(*m*-phthaloyl)-pentapeptides **9a**,**b**, **10a**,**b** and **11a**,**b**.

Because of the considerations that have been mentioned above and in addition to the continuing recent research interest in synthetic anticancer cyclopeptides herein, we aimed to synthesize some novel cyclo-(*m*-phthaloyl)-*bis*-[*L*-Phe -Gly/Sar]-*L*-Lys–X, where, X = COOMe (**9a**,**b**), COOH (**10a**,**b**) and $NHNH_2$ (**11a**,**b**) (Figure 1) to evaluate their anticancer potency against eight human cancer cells. The suggestion of glycine or sarcosine as alternating amino acids in the lateral cyclo-pentapeptide skeletal chain was derived from the manifested variation in their side groups' steric hindrance, namely, the simple for glycine and the bulkier for sarcosine. Such variations could permit the probing of the molecular interaction with their hypothetical biological receptor that allows structure-activity relationship investigations.

RESULTS AND DISCUSSION

Chemistry

Synthesis of *m*-phthaloyl-bis-[L-phenylalaninemethyl ester] and m-phthaloyl-bis-[L-phenylalanine], (**3**, **4**), respectively, were prebeared by Moustafa *et al.* [16]. Next, treatment of compound **4** with methyl ester of glycine **5a** as well as sarcosine **5b**, in the existence of ECF, yielded the matching *m*-phthaloyl-*bis*-(dipeptide)-esters **6a**,**b**, respectively. The hydrolyses of the latter methyl esters **6a**,**b** with NaOH gave the corresponding free acids *m*-phthaloyl-bis-(dipeptides) **6** and **7**, respectively (Scheme 2).

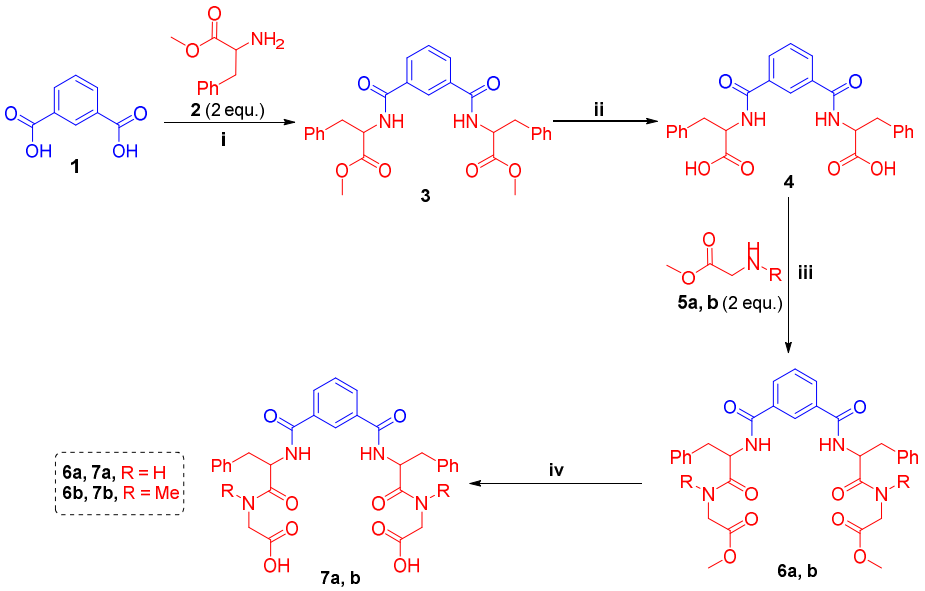

Scheme 1. Reagents and conditions: (**i**) Ethyl chloroformate (ECF), TEA (2 equ.), DCM, stirring 30 min at -20 ºC and 24 h at rt; (**ii**) (a) 1.0 N NaOH, MeOH, stirring 3 h at -20 ºC and 24 h at rt, (b) 1.0 N HCl; (**iii**) ECF, N-methylmorpholine (NMM) (2 equ.), DCM, stirring 30 min at -20 ºC and 24 h at rt; (**iv**) (a) 1.0 N NaOH, MeOH, stirring 3 h at -20 ºC and 24 h at rt, (b) 1.0 N HCl.

Cyclization of the *bis*-dipeptides **7a**,**b** with methyl ester of *L*-lysine **8** by using two different peptide coupling methods yielded the corresponding cyclo-pentapeptides cyclo-[*m*-phthaloyl-bis-(*L*-Phe-Gly/Sar)-*L*-Lys]-COOMe **9a**,**b**, respectively, in acceptable yield (Scheme 2). ^{1}H NMR spectrum of **9a**, **b** showed the appearance of the singlet signal of ester CH_3 group around δ 3.56 *ppm*, the signals of 3CH_2 of γ, δ and β-CH_2 of Lys around δ 1.50 ppm, in addition to the signals of α-CH and ε-CH_2 of Lys. The ^{13}C NMR of compound **9a**,**b** exhibited the existence of a signal at δ 54.8 ppm of CH_3.ester, an up-field signal around δ 174.0 ppm of ester C=O group in addition to the CH and 4CH_2 carbon signals of Lys.

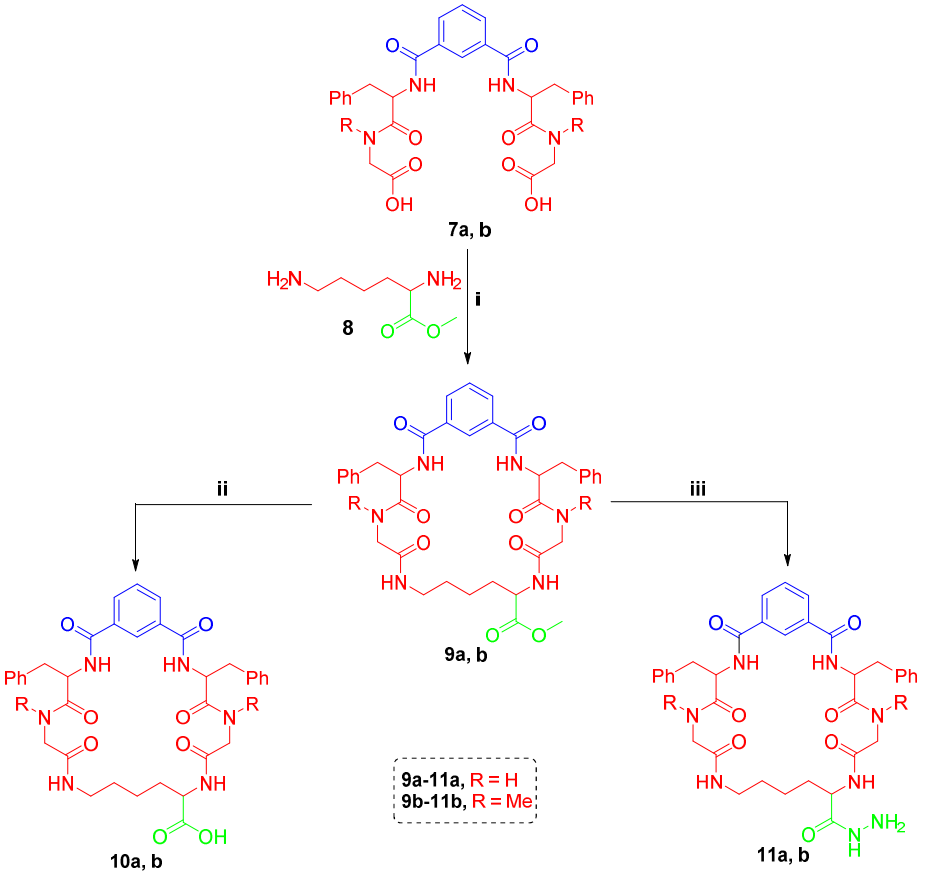

Scheme 2. Reagents and conditions: (**i**) (Method A) ECF, TEA (2 equ.), DCM, stirring 30 min at -15 ºC and 12 h at rt, (Method B) dicyclohexylcarbodiimide (DCC), THF, stirring, 20 h rt; (**ii**) (a) 1.0 N NaOH, MeOH, stirring 3 h at -20 ºC and 24 h at rt, (b) 1.0 N HCl; (**iii**) $NH_2NH_2.H_2O$ (99%), MeOH, reflux, 3 h.

Furthermore, the alkali hydrolysis using 1.0 *N* NaOH solution in methanol of cyclo-pentapeptide esters **9a**,**b** afforded to the corresponding acids cyclo-[*m*-phthaloyl-bis-(*L*-Phe-Gly/Sar)-*L*-Lys]-COOH **10a**,**b**, respectively (Scheme 2). The IR spectra of compound **10a** showed the absorption band of acidic carbonyl at 1718 and 1685 cm^{-1}, in addition to the absorption bands

of amidic carbonyl at 1684 and 1634 cm^{-1}, respectively. In contrast, their ^1H NMR spectra of compounds exhibited the D_2O exchangeable signal of carboxylic OH at δ 12.55 and 12.57 ppm, respectively.

Finally, hydrazinolysis of **9a**,**b** with methanolic hydrazine hydrate afforded the corresponding cyclo-pentapeptiedie hydrazides cyclo-[*m*-phthaloyl-bis-(*L*-Phe-Gly/Sar)-*L*-Lys]-$NHNH_2$ **11a**,**b**, respectively (Scheme 2). The IR spectra of compounds **11a** and **b** showed absorption bands in the range of 3440-3100 cm^{-1} due to NHs and hydrazide NH_2. ^1H NMR of compounds **11a**,**b** showed the D_2O exchangeable of hydrazide NH signals at δ 9.37 and 7.88 ppm. Respectively, in addition to the signals of hydrazide NH_2 at 3.93 and 3.43 ppm, respectively.

Anticancer activity

The cytotoxicity in this study is evaluated by the "Egyptian National Cancer Institute, Cairo, Egypt". Determination of the potential cytotoxicity (IC_{50}, µg/mL) for five cyclo-pentapeptides **9a**,**b**, **10a**,**b**, **11a**,**b,** and doxorubicin® as reference drug is assayed on 8 human tumor cell lines namely; "Human cancer cell lines breast *MCF-7* and *T47D*, liver *HEPG2*, colon *HCT116*, cervical cell line *HELA*, larynx *HEP2*, Prostate *PC3*, and intestinal *Caco*", and the data is represented in (Table 1). Considering the general cytotoxic activity profile upon targeting the tested 8 human tumor cell lines, the candidates **9a**, **9b**, **10a**, **11a** and **11b** showed moderate anticancer activity when compared with doxorubicin® whereas "cyclo-[*m*-phthaloyl-*bis*–(L-Phe-Sar)-L–Lys]-OH" **12**, exhibited excellent anticancer activity when compared with doxorubicin® (Table 1).

Table 1. Cytotoxicity (IC_{50}, µg/mL) of cyclo-pentapeptides **9a**,**b**, **10a**,**b**, **11a**,**b** and dxorubicin® as reference drug against eight human cell lines for cancer.

Comp-ound	IC_{50} (µg/mL)							
	MCF-7	*T47D*	HEPG2	*HCT116*	*HELA*	*HEP2*	*PC3*	*Caco*
9a	16.7	44.9	16.70	13.7	18.7	7.28	32.3	17.0
9b	4.35	6.83	14.60	9.68	14.00	15.20	8.40	10.10
10a	8.61	17.3	6.80	8.63	8.63	4.13	9.83	8.63
10b	2.97	4.28	2.97	4.13	3.20	3.20	4.80	3.83
11a	19.00	18.10	20.20	12.4	20.50	10.30	23.50	21.20
11b	16.10	10.40	16.50	9.53	14.30	14.00	9.98	11.80
Dox	2.97	7.80	3.73	3.73	4.19	3.73	4.80	3.58

Compound **10b** showed IC_{50} = 4.28, 2.97, 3.20, and 3.20 µg/mL against cell lines *T47D*, *HEPG2*, *HELA*, and *HEP2*, respectively, which are higher than those of doxorubicin® (7.80, 3.73, 4.19 and 3.73 µg/mL). In addition, compound **10b** revealed the same anticancer activity when compared with doxorubicin® toward *MCF-7* and *PC3* with IC_{50} = 2.97 and 4.80 µg/mL, respectively. Furthermore, Compound **10b** exhibited much closed IC_{50} values (4.13 and 3.83 µg/mL) when compared with doxorubicin® (IC_{50} = 3.73 and 3.58 µg/mL) against *HCT116* and Caco cell lines, respectively.

Molecular dynamic and system stability

To model and anticipate the behavior of the synthesized derivatives after attaching to the binding site of the receptor protein, and its interaction and stability, a molecular dynamic simulation was performed [28, 29]. The stability of the system needs to be verified in order to locate disturbed motions and keep simulation artifacts at a distance. In this current study, the "root-mean-square deviation" (RMSD) throughout the 20 ns simulations was used to gauge the stability of the systems. The all frames mean of RMSD for the **10b**-complex systems and apo-protein were, respectively, 2.06 Å and 2.61 Å (Figure 2A). These findings showed that, in comparison to the

other systems under study, the **10b**-linked to a complicated protein system developed a comparatively stronger conformation.

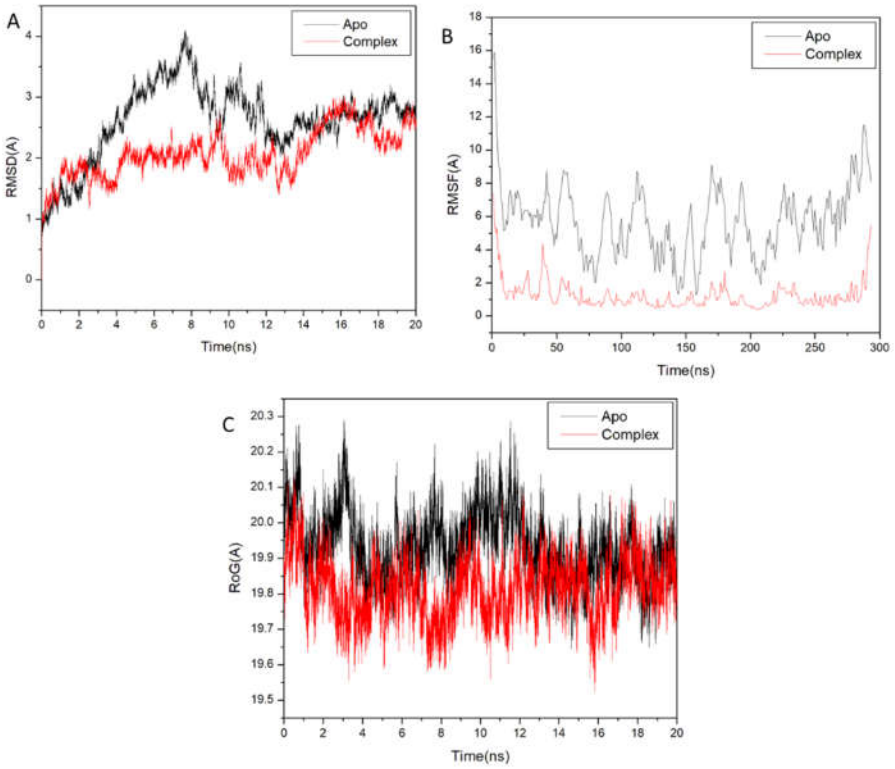

Figure 2. [A] RMSD of Cα atoms of the protein backbone atoms. [B] RMSF of each residue of the protein backbone Cα atoms [c] RoG of Cα atoms of protein residues of the backbone atoms relative (black) to the starting minimized over 20 ns for the EGFRKs protein with ligand **10b** (red).

To ensure that the residual behavior and its relationship to the binding site are analyzed during MD simulation, it is imperative to assess protein structural flexibility upon ligand binding [30]. Protein residue changes were measured using the root-mean-square fluctuation (RMSF) technique throughout a 20 ns simulation period in order to evaluate the influence of receptor blockers on the appropriate sites. The computed average RMSF values for **10b**-complex systems and apo-protein systems were 1.27 Å and 5.77 Å, correspondingly. The whole residue fluctuations of several routines are shown in Figure 2B. The results showed that compared to other systems, the **10b**-linked to a complicated protein system exhibited an inferior level of residual variation. The radius of gyration (Rg) provides information about the protein's structural compactness and simulated stability, (Figure 2C) shows the Rg outcomes for the complex and apo-protein with chemical **10b**, which were 19.810.08 Å and 19.930.09 Å, correspondingly. It was found that the structure of Rg of 12-bonded proteins is less stiff than that of Apo-protein.

Binding interaction mechanism based on binding free energy calculation

Molecular mechanics energy methodology (MM/GBSA) is a widely used approach for calculating the free binding energies of small molecules to biological macromolecules. It combined the surface area continuum solvation and generalized Born solvation techniques [31]. Using trajectory snapshots of the systems, the binding free energies were found using AMBER18's MM-GBSA tool. With the exception of G_{solv}, all of the reported calculated energy components have substantial negative values, which indicate beneficial interactions, as shown in (Table 2). The findings demonstrated that the **10b**-complex system's binding affinity was -16.59 kcal/mol.

Table 2. The calculated energy binding for compound **10b** against the epidermal growth factor receptor protein receptor.

Compound	Energy Components (kcal/mol)*				
	ΔE_{vdW}	ΔE_{elec}	ΔG_{gas}	ΔG_{solv}	ΔG_{bind}
10b	-40.15 ± 0.35	-22.92± 0.81	-17.22± 1.07	6.38 ± 0.074	-16.59 ± 0.33

*ΔE_{vdW} = van der Waals energy; ΔE_{elec} = electrostatic energy; ΔG_{solv} = solvation free energy; ΔG_{bind} = calculated total binding free energy.

A comprehensive analysis of each individual energy contribution, which results in the reported binding free energies, demonstrates that the more positive Vander Waals energy component drives the interactions between compound **10b** and the epidermal growth factor protein receptor residues (Table 2).

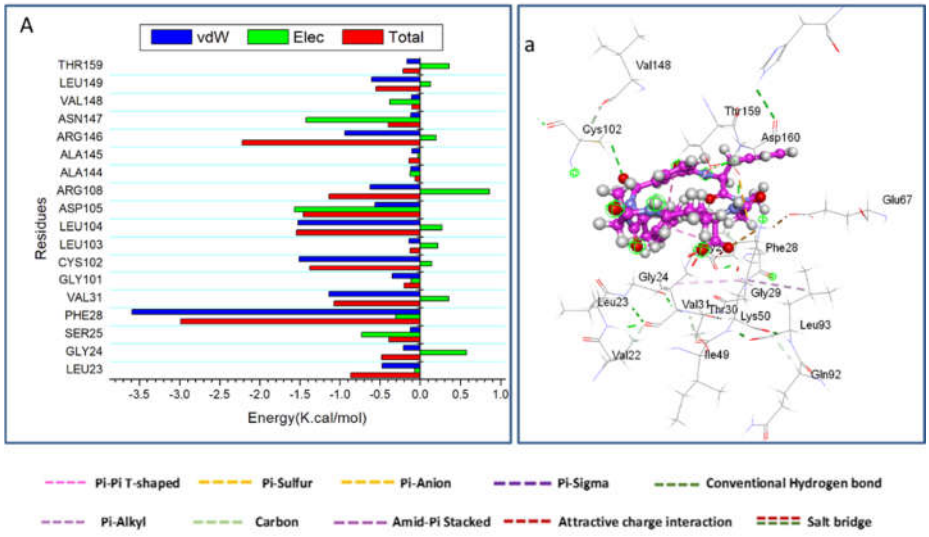

Figure 3. Compound **10b**'s per-residue breakdown graphs illustrate the energy contributions to the attaching and stabilization at the catalytic active site of the receptor for epidermal growth factor.

Identification of the critical residues responsible for ligand binding

To find out more about the important residues that are involved in the inhibition of the EGF receptor, the total energy involved when compound **10b** contacts the epidermal growth factor

receptor was further broken down into the association of particular site residues. From (Figure 3), the primary advantageous contribution of **10b** to EGFR receptor is mostly witnessed from Leu23 (-0.47), Gly24 (-0.20), Phe28 (-3.59), Val31 (-1.13), Gly101 (-0.348), Cys102 (-1.50), Leu103 (-0.13), Leu104 (-1.521), Asp105 (-0.563), Arg108 (-0.624), Arg146 (-0.941), Leu149 (-0.606) and Thr159 (-0.164) kcal/mol.

EXPERIMENTAL

Chemistry

Melting points were determined by using a digital thermoelectric instrument. R_f value was calculated using a mixture of n-hexane: ethyl acetate (3:1). Using thin layer chromatography (TLC). Infrared spectra (KBr, cm^{-1}) were measured on an IR 5300 Berkin Elmar spectrometer. The mass spectra were measured using GC MS-QP 1000 at 70 eV using the electron impact (EI) technique. Conductivity measurements in solution were performed using the TDS 72 conductivity model. "^{1}H NMR and ^{13}C NMR Spectra were run on Jeol instruments (JöEL 500 MHz, δ, ppm, DMSO-d_6)".

Synthesis of *m*-phthaloyl-bis-[L-phenylalaninemethyl ester] and *m*-phthaloyl-bis-[L-phenylalanine], (3, 4), respectively, were prebeared by Moustafa *et al* [16].

*Synthesis of m-phthaloyl-bis[dipeptide methyl ester] derivatives **6a, b***

These compounds were prepared using the same method of the synthesis of compound **3** by the reaction of *m*-phthaloyl-*bis*-[*L*-phenylalanine] **4** with methyl glycinate (**5a**) or sarcosine methyl ester (**5b**) using *N*-methylmorpholine (NMM) instead of TEA to give the corresponding esters **6a**, **b**, respectively.

6a. Yield: 55%; m.p. 109-112 °C, $[\alpha]_D^{25}$: -3.2 (C, 0.07, MeOH). IR (ν, cm^{-1}): 3429 (NHs), 2980 (CH aromatic), 2362 (CH aliphatic), 1642 (C=O ester), 1449 (C=O amide). MS (*m/z*, %): 633 (M^++2, 22.36). Elemental analysis for $C_{34}H_{38}N_4O_8$ (630.69); calculated: C 64.75, H 6.07, N 8.88; found: C 64.80, H 6.18, N 8.90.

6b. Yield: 70%; m.p. 116-119 °C.; $[\alpha]_D^{25}$: -18.5 (C, 0.08, MeOH). IR (ν, cm^{-1}): 3409 (NHs), 2943 (CH group of the aromatic ring), 2539 (CH group of the aliphatic chain), 1744 (C=O of the ester), 1698 (C=O bond of the amide). MS (*m/z*, %): 631 (M^+, 6.37). Elemental analysis for $C_{34}H_{38}N_4O_8$ (630.7); calculated: C 64.75, H 6.07, N 8.88; found: C 64.88, H 6.19, N 9.00.

*Synthesis of m-phthaloyl-tetrapeptide derivatives **7a**,**b***

These compounds were prepared using the same method for the synthesis of ester **4** by using esters **6a**,**b**, instead of ester **3** to present the matching tetrapeptides **7b**, correspondingly.

7a. Yield: 66%; m.p. 118-120 °C.; $[\alpha]_D^{25}$: -9.1 (C, 0.02, MeOH). IR (ν, cm^{-1}): 3383 (NH), 3029 (CH group of the aromatic ring), 2925 (CH group of the aliphatic chain), 1719 (C=O bond of the acid), 1671 (C=O bond of the amide). MS (*m/z*, %): 575 (M^+, 93.40). Elemental analysis for $C_{30}H_{30}N_4O_8$ (574.6). Calculated: C 62.71, H 5.26, N 9.75. Found: C 62.60, H 5.20, N 9.80.

7b. Yield: 40%; m.p. 127-130 °C.; $[\alpha]_D^{25}$: -18.2 (C, 0.08, MeOH). IR (ν, cm^{-1}): 3394 (NH stretching), 3030 (CH group of the aromatic ring), 2926 (CH group of the aliphatic chain), 1720 (C=O bond of the acid), 1525 (C=O bond of the amide). MS (*m/z*, %): 603 (M^++1, 0.32). Elemental analysis for $C_{32}H_{34}N_4O_8$ (602.2). Calculated: C 63.78, H 5.69, N 9.30. Found: C 63.85, H 5.55, N 9.15.

*Synthesis of cyclo-cyclo pentapeptide methyl esters **9a**,**b***

Method A: mixed anhydride method

Ethyl chloroformate (ECF) (0.2 mL, 2 mmol) was supplemented drop-wise within 30 min to a chilled, agitated mixture (-15 ºC) of the appropriate *m*-phthoyl-*bis* (dipeptide) **7a**,**b** (1 mmol) and TEA (0.2 mL, 2 mmol) in DCM (20 mL). The reaction mixture was stirred for an additional 30 min., and then an icy solution (-15 ºC) of methyl ester of *L*-lysine (**8**) (1.0 mmol) in DCM (20 mL) was added within 30 min. Mixing was preserved for three hours at -15 ºC and half a day at an ambient temperature. The reactive mix was bathed with H_2O, 1.0 *N* Na_2CO_3, 1.0 *N* $KHSO_4$, and H_2O then dehydrated over anhydrous Na_2SO_4. After the solvent was evaporated under low pressure until it was completely dry, the oily residual was triturated with a dry ether/n-hexane combination to solidify it. Preparative thin-layer chromatography was used to purify the crude product, yielding the corresponding cyclic pentapeptide methyl esters, **9a**,**b**, by utilizing S_3 as the eluent.

Method B: DCC method

To a cold solution (-5 ºC) of methyl ester of *L*-lysine (1 mmol) and the appropriate acid **7a**,**b** (1 mmol) in THF (40 mL), a solution of dicyclohexylcarbodiimide (DCC) (0.42 g, 2 mmol) in THF (20 mL) was then gradually added over a 20-min period at the same degree of temperature. The mixture was kept at room temperature for twenty hours. After adding 20 mL of acetonitrile to the reaction mixture, the resulting dicyclohexylurea was filtered out and given another acetonitrile wash (2x10 mL). After an overnight refrigeration of the filtrate, the freshly produced dicyclohexylurea was filtered out. THF was evaporated until it was completely dry, after which the residue was dissolved in DCM, washed with water, 1.0 *N* $KHSO_4$, and Na_2CO_3, and then dried over anhydrous Na_2SO_4. After the solvent was evaporated entirely, the oily residue was triturated with a dry ether/n-hexane combination to solidify it. The resulting solid was filtered and precipitated to provide the cyclic pentapeptide methyl esters **9a, b** from the EtOH/n-hexane combination. Melting point analysis and TLC were used to identify esters **9a** and **9b** by comparing them to genuine samples made using procedure A.

9a. Yield (%) 81 [method A], 60 [method B]; m.p. 116-119 ºC, $[\alpha]_D^{25}$: -18 (C, 0.02, MeOH). IR (ν, cm^{-1}): 3428 (NHs), 2995 (CH group of the aromatic ring), 2912 (CH group of the aliphatic chain), 1656 (C=O bond of the ester), 1433 (C=O bond of the amide). ^{1}H NMR δ: 8.63 (m, 1H, H_2 of phthaloyl), 8.14-8.13 (m, 2H, H_4 and H_6 of phthaloyl), 8.12 (s, D_2O exchangeable, 6H, 6NH, amidic NHs), 7.60 (m, 1H, H_5 of phthaloyl), 7.22-7.21 (m, 10H, 2Ph), 4.92 (t, 2H, 2NHC<u>H</u>C<u>H</u>$_2$Ph), 4.59 (t, 1H, α CH of Lys), 4.31-4.27 (s, 4H, 2CH_2, 2NHC<u>H</u>$_2$CO of Gly), 3.56 (s, 3H, COOC<u>H</u>$_3$), 3.34 (d, 4H, 2C<u>H</u>$_2$Ph), 3.15-3.13 (m, 2H, 2ε-CH_2 of Lys), 2.21-1.25 (m, 6H, 3CH_2, γ, δ, β-CH_2 of Lys). ^{13}C NMR δ: 39.9, 39.7, 39.5 (3C, γ, δ and β-C<u>H</u>$_2$ of Lys), 40.3, 40.2 (2C<u>H</u>$_2$-NH), 40.5 (ε-C<u>H</u>$_2$ of Lys), 54.8 (COOC<u>H</u>$_3$), 60.2 (α-C<u>H</u> of Lys), 60.3 (2NHC<u>H</u>CH_2Ph), 126.9 (2C), 128.7, 128.5 (2C), 129.5 (2C), 129.7 (2C), 130.3 (2C), 130.5 (2C), 133.9 (2C), 157, 156.8 (2NHC<u>O</u>Ph), 167.1 (2NHC<u>O</u>CH), 173.6 (2NHC<u>O</u>CH_2), 174.6 (C<u>O</u>OCH_3). MS (*m/z*, %): 699 (M^++1, 17.85). Elemental analysis for $C_{37}H_{42}N_6O_8$ (698.8); calculated: C 63.60, H 6.06, N 12.03; found: C 63.69, H 6.04, N 11.95.

9b. Yield (%) 75 [A], 55 [B]; m.p. 130-132 ºC, $[\alpha]_D^{25}$: -6.6 (C, 0.25, MeOH). IR (ν, cm^{-1}): 3434 (NHs), 2953 (CH group of the aromatic ring), 2840 (CH group of the aliphatic chain), 1650 (C=O bond of the ester), 1455 (C=O bond of the amide). ^{1}H NMR δ: 8.63-8.61 (m, 1H, H_2 phthaloyl), 8.30-8.00 (m, 2H, H_4 and H_6 phthaloyl), 7.95, 7.85 (2s, D_2O exchangeable, 2H, 2NH), 7.85-7.80

(m, 1H, H_5 phthaloyl), 7.45-7.39 (m, 4H, $2H_3$ and $2H_5$ of 2Ph), 7.35-7.31 (m, 4H, $2C_2$ and $2C_6$ of 2Ph), 7.23-7.19 (m, 2H, $2H_4$ of 2Ph), 4.40 (t, 2H, 2NHCHCH$_2$Ph), 3.85 (t, 1H, α-CH of Lys), 3.57 (s, 6H, $2CH_3$, $2NCH_3$), 3.56 (s, 3H, COOCH$_3$), 3.55 (dd, 4H, $2CH_2$Ph), 3.21 (s, 4H, $2CH_2$, $2NCH_3CH_2CO$ of 2Sar), 3.20-2.80 (m, 2H, ε-CH_2 of Lys), 1.56-1.29 (m, 6H, $3CH_2$, γ, δ and β-CH_2, Lys). ^{13}C NMR δ: 23.2 (δ-CH_2 of Lys), 29.4 (γ-CH_2 of Lys), 30.9 (β-CH_2 of Lys), 40, 39.8 ($2NCH_3$), 40.2 (2NHCHCH_2Ph), 52.3 (ε-CH_2 of Lys), 52.9 ($COOCH_3$), 54.3 (2NHCHCH$_2$Ph), 59.9 (2NHCOCH_2), 60.5 (α-CH, Lys), 101.2 (2C), 128 (2C), 128.5 (2C), 129.6 (4C), 129.8, 129.7 (2C), 139.9 (2C), 149.9 (2C=O), 166.3, 165.8, 165.7, 156.8 (4C=O), 173.6 ($COOCH_3$). MS (*m/z*, %): 727 (M^+, 20.27). Elemental analysis for $C_{39}H_{46}N_6O_8$ (726.8); calculated: C 64.45, H 6.38, N 11.56; found: C 64.40, H 6.39, N 11.71.

Synthesis of cyclo-pentapeptides ***10a,b***

Sodium hydroxide (1.0 N, 25 mL) was progressively added to a stirred and cold methanolic solution (-5 °C, 20 mL) of the corresponding cyclo-pentapeptide methyl esters **(9a**,**b)**, respectively (1 mmol). After three hours at the same temperature, the reaction mixture was stirred for twenty-four hours at ambient temperature. After the solvent was removed by distillation at low pressure, the leftover aqueous solution was cooled and treated with 1.0 N hydrochloric acid (pH about 3). To get the matching cyclo-pentapeptides **10a** and **b**, the resulting solid was filtered out, washed with water, dried, and crystallized from ethanol/water.

10a. Yield: 70%; m.p. 144-147 °C, $[\alpha]_D^{25}$: -29.4 (C, 0.02, MeOH). IR (ν, cm^{-1}): 3376 (NHs), 2926 (CH group of the aromatic ring), 2857 (CH group of the aliphatic chain), 1718 (C=O bond of the acid), 1684 (C=O bond of the amide). ^{1}H NMR δ: 12.55 (s, D_2O exchangeable, 1H, OH), 8,07, 8.03 (2s, D_2O exchangeable, 6H, 6NH), 7.93-7.10 (m, 14H, ArHs), 4.33-4.30 (m, 3H, 2NHCHCH$_2$, Ph + 1H, α-CH of Lys), 3.92-3.65 (m, 8H, $4CH_2$, $2CH_2$, Ph + 2NHCH_2CO), 2.30-1.74 (m, 6H, $3CH_2$, γ-, δ- and β-CH_2 of Lys). MS (*m/z*, %): 685 (M^+, 0.24). Elemental analysis for $C_{36}H_{40}N_6O_8$ (684.7); calculated: C 63.15, H 5.89, N 12.27; found: C 63.20, H 5.78, N 12.28.

10b. Yield: 75%; m.p. 163-165 °C, $[\alpha]_D^{25}$: -7.3 (C, 0.25, MeOH). IR (ν, cm^{-1}): 3407 (NHs), 2922 (CH group of the aromatic ring), 2859 (CH group of the aliphatic chain), 1685 (C=O bond of the acid), 1634 (C=O bond of the amide). ^{1}H NMR δ: 12.57 (s, 1H, OH, D_2O exchangeable), 8.26-8.24 (m, 3H, H_2, H_4 and H_6 phthaloyl), 7.70 (s, 5H, 4NH, D_2O exchangeable + H_5 of phthaloyl), 7.21 (m, 4H, $2H_3$ and $2H_5$ of 2Ph), 7.16-7.15 (m, 4H, $2H_2$ and $2H_6$ of 2Ph), 7.13-7.10 (m, 2H, $2H_4$ of 2Ph), 4.35 (t, 2H, 2NHCHCH$_2$Ph), 4.30 (t, 1H, α-CH of Lys), 3.94 (s , 4H, $2CH_2$ of Sar), 3.51 (s, 6H, $2CH_3$, $2NCH_3$), 3.27 (dd, 4H, 2NHCHCH$_2$Ph), 3.26-3.24 (m, 2H, ε-CH_2 of Lys), 1.94-1.10 (m , 6H, $3CH_2$, γ, δ and β-CH_2 of Lys). ^{13}C NMR δ: 22.9 (δ-CH_2 of Lys), 29.6 (γ-CH_2 of Lys), 30.8 (β-CH_2 of Lys), 40, 39.8 ($2NCH_3$), 40.2, 40.00 (2NHCHCH_2Ph), 51.50 (ε-CH_2 of Lys), 52.5, 51.7 (2NHCHCH$_2$Ph), 61.3, 60.4 (2NHCOCH_2), 61.50 (α-CH, Lys), 128.5, 128.7 (4C), 129.6, 130.3 (4C), 135.5 (2C), 138.5 (2C), 156.8, 156.3 (2C), 171.5, 170.9, 170.6, 157.1 (2 NHC=O + 2 NCH_3C=O), 173.9 (COOH). MS (*m/z*, %): 713 (M^++1, 0.17). Elemental analysis for $C_{38}H_{44}N_6O_8$ (712.8); calculated: C 64.03, H 6.22, N 11.79; found: C 64.13, H 6.34, N 11.80.

Synthesis of cyclo-pentapeptide hydrazides ***11a,b***

Hydrazine hydrate (99%, 0.35 mL, 10 mmol) was added to a stirred methanolic solution (50 mL) containing the appropriate cyclic pentapeptide methyl esters **9a**,**b** (1 mmol). The solvent was removed from the reaction mixture after it had refluxed for three hours. The residue that was obtained underwent ether trituration, filtration, and crystallization from methanol/ether to produce the corresponding cyclic pentapeptide hydrazides **11a**,**b**.

11a. Yield: 70%; m.p.172-174 °C. $[\alpha]_D^{25}$: -76.3 (C, 0.02, MeOH). IR (ν, cm^{-1}): 34233100-(NHs+NH_2), 3000 (CH group of the aromatic ring), 2915 (CH group of the aliphatic chain), 1654 (C=O). ^1H NMR δ: 9.37 (s, D_2O exchangeable, 1H, CONHNH$_2$), 8.12 (m, 4H, phthaloyl), 7.82-7.79 (m, D_2O exchangeable, 4H, 4NH), 7.30-26 (m, 4 H, $2H_3$, $2H_5$ of 2Ph), 7.20 (m, 4H, $2H_2$ and $2H_6$ of 2Ph), 7.19-7.17 (m, 2H, $2H_4$ of 2Ph), 4.89 (t, 2H, 2NHCHCH$_2$Ph), 4.66 (t, 1H, α-CH of Lys), 3.93 (s, D_2O exchangeable, 2H, 2CONHNH$_2$), 3.81 (s, 4H, $2CH_2$ of 2α-Gly), 3.46 (dd,4 H, 2NHCHCH$_2$Ph), 3.02 (m, 2H, ε-CH_2 of Lys), 2.86-1.70 (m, 6H, $3CH_2$, γ-, δ- and β-CH_2 of Lys). MS (*m/z*, %): 699 (M^+, 11.32). Elemental analysis for $C_{36}H_{42}N_8O_7$ (698.8); calculated: C 61.88, H 6.06, N 16.04; found: C 61.89, H 6.26, N 16.05.

11b. Yield: 80%; m.p. 222-224 °C, $[\alpha]_D^{25}$: -44 (C, 0.03, MeOH). IR (ν, cm^{-1}): 3440-3199 (NHs+NH_2), 3000 (CH group of the aromatic ring), 2960 (CH group of the aliphatic chain), 1641 (C=O). ^1H NMR δ: 7.88 (s, 5H, D_2O exchangeable, 1H, CONHNH$_2$ + 4H, 4NH amidic), 7.25-7.20 (m, 4H, phthaloyl + 10H, 2Ph), 4.63 (t, 2H, 2NHCHCH$_2$Ph), 3.91 (t, 1 H, α-CH of Lys), 3.43 (s, D_2O exchangeable, 2H, 2CONHNH$_2$), 3.40, 3.28 (s, 4H, $2CH_2$ of 2α-Sar), 3.17 (s, 6H, $2CH_3$, 2NCH$_3$), 2.90-2.85 (m, 2H, ε-CH_2 of Lys), 2.50, 2.46 (2d, 4H, 2NHCHCH$_2$Ph), 1.91-1.10 (m, 6H, $3CH_2$ of γ-, δ- and β-CH_2 of Lys). MS (*m/z*, %): 727 (M^+, 5.73). Elemental analysis for $C_{38}H_{46}N_8O_7$ (726.8); calculated: C 62.79, H 6.38, N 15.42; found: C 62.82, H 6.40, N 15.47.

Anticancer activity

The potential cytotoxicity of the cylcopentapeptides, **9-14**, was determined according to the colorimetric method described by Skehan *et al.* for anticancer, "drug screening" [32]. Eight types of human cancer cell lines (HCC), namely, *MCF-7*, *T47D*, *HEPG2*, *HCT116*, *HELA*, *HEP2*, *PC3*, and *Caco* and *DOX*® as reference drugs, were experimented. A 96-well microtiter plate was handled, and *Sulforhodamine*® (SRB) was used as the staining dye. The anticancer activity is evaluated using the apparatus ELISA Reader-Sunrise-TECAN. Cancer cells were placed in a 96-well microliter plate for 24 hours before treatment with freshly prepared peptides to allow cell attachment to the plate wall. Several different concentrations of the investigated compounds (0, 10, 25, 50, and 100 µg/mL) were added to the wells of the monolayer as well as the trilayer cells (at a constant rate of three wells per dose). Our compounds were incubated with cell monolayers for up to 48 hours at 37 °C in a mild atmosphere of 5% CO_2. Forty-eight hours later, all cells were treated with Sulfo-Rhodamine-B and 10% trichloroacetic acid (TCAA). On the other hand, the cells were washed with water to remove excess TCA, growth medium, low molecular weight metabolites, and serum proteins and were air-dried at last. Further, the cells are stained for 30 min using a 0.4% mixed solution of (w/v, SRB, 1% acetic acid solution). At the end of this period, the dye is rapidly removed up to 4 times with a 1% acetic acid solution. In order to measure a color intensity in an ELISA reader, the bound dye must be recovered, which is done by solubilization with a mixed solution of Tris/EDTA (ethylenediaminetetraacetic acid solution). A compound with very promising initial results is selected, then the relationship between the antibody surviving fraction and the drug concentration is plotted in order to be able to obtain a survival curve for each cancer cell line. IC_{50} (the concentration of the compound needed to kill 50% of the initial cells) was determined for each compound. Compounds with no practical IC_{50} (> 100 µg/mL) were considered as inactive. All results were expressed throughout as means +/- S.E.M.

Molecular dynamic

System preparation

The crystal structure of the human epidermal growth factor receptor tyrosine kinase enzymes was acquired from the protein data repository using the code 1M17 [33]. These structures were then

prepared for molecular dynamics (MD) studies using UCSF Chimaera [34]. Using PROPKA [35], the pH was set and tuned at 7.5. The 3e structure was produced using "ChemBioDraw Ultra" 12.1 [36]. According to the guidelines in the simulation section, 20 ns MD simulations were performed on each of the two constructed systems.

Molecular dynamic (MD) simulations

Due to the use of molecular dynamic (MD) simulations, the study of biological systems may now explore the physical motion of atoms and molecules in a way that is not currently conceivable using any other approach [37]. A nuanced view of the dynamical evolution of biological systems, including conformational changes and molecular interaction, is provided by the knowledge obtained by running this simulation [37]. All systems' MD simulations were performed on the GPU version of the PMEMD engine included in the AMBER 18 package [38]. Each chemical's partial atomic charge was ascertained using the General Amber Force Field (GAFF) approach from ANTECHAMBER [39]. Any system inside an orthorhombic box of TIP3P water molecules was implicitly solvated by the Leap module of the AMBER 18 package within 10 of any box edge. Using the Leap module, the systems were neutralized by introducing Na+ and Cl- counterions. Each system first had a 2000-step initial minimization with an applied constraint potential of 500 kcal/mol, and then it underwent a 1000-step full minimization using the conjugate gradient algorithm without any restrictions. Each system was gradually heated from 0 K to 300 K during a 500 ps interval in order to guarantee that all systems had the same number of atoms and volume during the MD simulation. The system's solutes were exposed to a 10 kcal/mol potential harmonic constraint and a 1 ps collision frequency. After that, each system was heated and maintained at a constant temperature of 300 K for 500 ps to reach equilibrium. The number of atoms and system pressure were held constant for each manufacturing simulation, with the system pressure being kept at 1 bar using the Berendsen barostat [40]. In order to model an isobaric-isothermal (NPT) ensemble, this was done. For 20 ns, each system underwent MD simulation. The SHAKE method was used to restrict the hydrogen bond atoms in each simulation. An SPFP precision model and a 2 fs step size were used in each simulation. "An isobaric-isothermal ensemble (NPT) with randomized seeding, a constant pressure of 1 bar, a pressure-coupling constant of 2 ps, a temperature of 300 K, and a Langevin thermostat with a collision frequency of 1 ps were all used in the simulations".

Post-MD analysis

The CPPTRAJ [41] module of the AMBER18 suite was used to analyze the trajectories after MD simulations had saved them at intervals of 1 ps. All graphs and visualizations were made using Chimaera and the data analysis program Origin [42, 43].

Thermodynamic calculation

The "Poisson-Boltzmann or generalized Born and surface area continuum solvation (MM/PBSA and MM/GBSA)" approach has been shown to be useful for estimating ligand-binding affinities [44-46]. Within a predefined force field, the MM/GBSA and MM/PBSA protein-ligand complex molecular simulations calculate precise statistical-mechanical binding free energies. The average of more than 200 images from the whole 20-ns flight was used to calculate the binding free energy. The estimation of the change in binding free energy (G) for each molecular species (complex, ligand, and receptor) can be demonstrated as follows [47]:

$$\Delta G_{bind} = G_{complex} - G_{receptor} - G_{ligand} \quad (1)$$

$$\Delta G_{bind} = E_{gas} + G_{sol} - TS \quad (2)$$

$$E_{gas} = E_{int} + E_{vdw} + E_{ele} \quad (3)$$

$$G_{sol} = G_{GB} + G_{SA} \quad (4)$$

$$G_{SA} = \gamma SASA \quad (5)$$

Internal energy, van der Waals energy, Coulomb energy, and gas-phase energy are denoted by the abbreviations E_{gas}, E_{int}, E_{ele}, and E_{vdw}, respectively. The E_{gas} was calculated directly using the FF14SB force field terms. Calculating the solvent-free energy (G_{sol}) utilized the energy from the polar states (G_{GB}) and non-polar states (G). The non-polar solvation-free energy (G_{SA}) was computed from the solvent-accessible surface area (SASA) using a water probe radius of 1.4 [48, 49]. The polar solvation (G_{GB}) contribution, in contrast, was assessed by resolving the GB equation. The solute's temperature and total entropy are denoted by the letters S and T, respectively.

CONCLUSION

To conclude, our initial hypothesis that "cyclo-pentapeptides" of the structure "cyclo-(*m*-phthaloyl)-*bis*-[*L*-Phe -Gly/Sar]-*L*-Lys–X", where X = COOMe (**9a**,**b**), COOH (**10a**,**b**) and $NHNH_2$ (**11a**,**b**), as possible potent anticancer candidates, seemed validated. Targeting the tested eight human cancer cell lines, compound **10b**, cyclo-[*m*-phthaloyl-*bis*-(*L*-Phenylalanyl-Sarcosyl)-*L*–Lysine]-COOH, exhibited an excellent anticancer activity when compared with doxorubicin as reference drug. The novel designed and synthesized candidates, prospectively, merit further pronounced, in *vivo*, investigations on animal experimental models. Biological mechanistic studies, practically as epigenetic histone deacetylase inhibitor*s,* have strong rationales herein. Such studies are currently in progress.

ACKNOWLEDGMENT

Authors are grateful to King Saud University, Riyadh, Saudi Arabia for funding the work through Researchers Supporting Project No. (RSP2024R359).

REFERENCES

1. Esfahani, K.; Roudaia, L.; Buhlaiga, N.A.; Del Rincon, S.V.; Papneja, N.; Miller, W.H. A review of cancer immunotherapy: from the past, to the present, to the future. *Curr. Oncol.* **2020**, 27, 87-97.
2. Tsimberidou, A.M.; Fountzilas, E.; Nikanjam, M.; Kurzrock, R. Review of precision cancer medicine: Evolution of the treatment paradigm. *Cancer Treat Rev.* **2020**, 86, 102019.
3. Maruthappu, M.; Watkins, J.; Noor, A.M.; Williams, C.; Ali, R.; Sullivan, R.; Zeltner, T.; Atun, R. Economic downturns, universal health coverage, and cancer mortality in high-income and middle-income countries, 1990–2010: a longitudinal analysis. *Lancet.* **2016**, 388, 684-695.
4. Rosen, E.; Drilon, A.; Chakravarty, D. Precision oncology: 2022 in review. *Cancer Discov.* **2022**, 12, 2747-2753.
5. Siegel, R.L.; Miller, K.D.; Fuchs, H.E.; Jemal, A. Cancer statistics, 2021. *CA Cancer J. Clin.* **2021**, 71, 7-33.
6. Ramadhani, D.; Maharani, R.; Gazzali, A.M.; Muchtaridi, M. Cyclic peptides for the treatment of cancers: A review. *Molecules* **2022**, 27, 4428.
7. Zhang, J.N.; Xia, Y.X.; Zhang, H.J. Natural cyclopeptides as anticancer agents in the last 20 years. *Int. J. Mol. Sci.* **2021**, 22, 3973.

8. Moustafa, G.O.; Younis, A.; Al-Yousef, S.A.; Mahmoud, S.Y. Design, synthesis of novel cyclic pentapeptide derivatives based on 1,2-benzenedicarbonyl chloride with expected anticancer activity. *J. Comput. Theor. Nanos.* **2019**, 16, 1733-1739.
9. Naglah, A.M.; Moustafa, G.O.; Elhenawy, A.A.; Mounier, M.M.; El-Sayed, H.; Al-Omar, M.A.; Almehizia, A.A., Bhat, M.A. N^{α}-1,3-Benzenedicarbonyl-bis-(amino acid) and dipeptide candidates: synthesis, cytotoxic, antimicrobial and molecular docking investigation. *Drug Des. Dev. Ther.* **2021**, 15, 1315-1332.
10. Moustafa, G.O.; Shalaby, A.; Naglah, A.M.; Mounier, M.M.; El-Sayed, H.; Anwar, M.M.; Nossier, E.S. Synthesis, characterization, in vitro anticancer potentiality, and antimicrobial activities of novel peptide–glycyrrhetinic-acid-based derivatives. *Molecules* **2021**, 26, 4573.
11. Khalaf, H.S.; Naglah, A.M.; Al-Omar, M.A.; Moustafa, G.O.; Awad, H.M; Bakheit, A.H. Synthesis, docking, computational studies, and antimicrobial evaluations of new dipeptide derivatives based on nicotinoylglycylglycine hydrazide. *Molecules* **2020**, 25, 3589.
12. Moustafa, G.O. Therapeutic potentials of cyclic peptides as promising anticancer drugs. *Egypt. J. Chem*. **2021**, 64, 1777-1787.
13. Abd El-Meguid, E.A.; Naglah, A.M.; Moustafa, G.O.; Awad, H.M.; El Kerdawy, A.M. Novel benzothiazole-based dual VEGFR-2/EGFR inhibitors targeting breast and liver cancers: Synthesis, cytotoxic activity, QSAR and molecular docking studies. *Bioorg. Med. Chem. Lett.* **2022**, 58, 128529.
14. Mohamed, F.H.; Shalaby, A.; Abdelazem, A.; Mounier, M.; Nossier, E.S.; Moustafa, G.O. Design, synthesis and molecular docking studies of novel cyclic pentapeptides based on phthaloyl chloride with expected anticancer activity. *Egypt. J. Chem.* **2020**, 63, 1723-1736.
15. Abo-Ghalia, M.H.; Moustafa, G.O.; Amr, A.E.; Naglah, A.M.; Elsayed, E.A.; Bakheit, A.H. Anticancer activities of newly synthesized chiral macrocyclic heptapeptide candidates. *Molecules* **2020**, 25, 1253.
16. Moustafa, G.O.; Sabry, E.; Zayed, E.M.; Mohamed, G.G. Structural characterization, spectroscopic studies, and molecular docking studies on metal complexes of new hexadentate cyclic peptide ligand. *Appl. Organomet. Chem.* **2022**, 36, e6515.
17. Kalmouch, A.; Rdwan, M.; Omran, M.; Sharaky, M.; Moustafa, G.O. Synthesis of novel 2, 3'-bipyrrole derivatives from chalcone and amino acids as antitumor agents. *Egypt. J. Chem.* **2020**, 63, 4409-4421.
18. Abd El-Meguid, E.A.; El-Deen, E.M.M.; Moustafa, G.O.; Awad, H.M.; Nossier, E.S. Synthesis, anticancer evaluation and molecular docking of new benzothiazole scaffolds targeting FGFR-1. *Bioorg. Chem.* **2022**, 119, 105504.
19. Humphrey, J.M.; Chamberlin, A.R. Chemical synthesis of natural product peptides: coupling methods for the incorporation of noncoded amino acids into peptides. *Chem. Rev.* **1997**, 97, 2243-2266.
20. Qian, Z.; Liu, T.; Liu, Y.Y.; Briesewitz, R.; Barrios, A.M.; Jhiang, S.M.; Pei, D. Efficient delivery of cyclic peptides into mammalian cells with short sequence motifs. *ACS Chem. Biol.* **2013**, 8, 423-431.
21. Szabó, I.; Yousef, M.; Soltész, D.; Bató, C.; Mező, G.; Bánóczi, Z. Redesigning of cell-penetrating peptides to improve their efficacy as a drug delivery system. *Pharmaceutics* **2022**, 14, 907.
22. McKeever, B.; Pattenden, G. Total synthesis of the cytotoxic cyclopeptide mollamide, isolated from the sea squirt *Didemnum molle*. *Tetrahedron* **2003**, 59, 2701-2712.
23. Napolitano, A.; Rodriquez, M.; Bruno, I.; Marzocco, S.; Autore, G.; Riccio, R.; Gomez-Paloma, L. Synthesis, structural aspects and cytotoxicity of the natural cyclopeptides yunnanins A, C and phakellistatins 1, 10. *Tetrahedron*. **2003**, 59, 51, 10203-10211.
24. Moustafa, G.O.; Al-Wasidi, A.S.; Naglah, A.M.; Refat, M. Synthesis of dibenzofuran derivatives possessing anticancer activities: A review. *Egypt. J. Chem.* **2020**, 63, 2355-2367.

25. Al-Wasidi, A.S.; Naglah, A.; Kalmouch, A.; Adam, A.M.A.; Refat, M.; Moustafa, G.O. Preparation of Cr_2O_3, MnO_2, Fe_2O_3, NiO, CuO, and ZnO oxides using their glycine complexes as precursors for in situ thermal decomposition. *Egypt. J. Chem.* **2020**, 63, 1109-1118.
26. Moustafa, G.O. Synthesis of dibenzofuran derivatives possessing anti-bacterial activities. *Egypt. J. Chem.* **2021**, 64, 2075-2093.
27. Vander Molen, K.M.; McCulloch, W.; Pearce, C.J.; Oberlies, N.H. Romidepsin (Istodax, NSC 630176, FR901228, FK228, depsipeptide): A natural product recently approved for cutaneous T-cell lymphoma. *J. Antibiot.* **2011**, 64, 525-531.
28. Ylilauri, M.; Pentikäinen, O.T. MMGBSA as a tool to understand the binding affinities of filamin–peptide interactions. *J. Chem. Inf. Model.* **2013**, 53, 2626-2633.
29. Hayes, J.M.; Archontis, G.; MM-GB (PB) SA calculations of protein-ligand binding free energies. *Mol. Dyn.: Stud. Synth. Biol. Macromol.* **2012**, 171-190.
30. Hou, T.; Wang, J.; Li, Y.; Wang, W.; Assessing the performance of the MM/PBSA and MM/GBSA methods. 1. The accuracy of binding free energy calculations based on molecular dynamics simulations. *J. Chem. Inf. Model.* **2011**, 51, 69-82.
31. Greenidge, P.A.; Kramer, C.; Mozziconacci, J.C.; Wolf, R.M. MM/GBSA binding energy prediction on the PDBbind data set: successes, failures, and directions for further improvement. *J. Chem. Inf. Model.* **2013**, 53, 201-209.
32. Kleeff, J.; Kornmann, M.; Sawhney, H.; Korc, M. Actinomycin D induces apoptosis and inhibits growth of pancreatic cancer cells. *Int. J. Cancer.* **2000**, 86, 399–407.
33. Mirzaei, S.; Eisvand, F.; Hadizadeh, F.; Mosaffa, F.; Ghasemi, A.; Ghodsi, R. Design, synthesis and biological evaluation of novel 5,6,7-trimethoxy-N-aryl-2-styrylquinolin-4-amines as potential anticancer agents and tubulin polymerization inhibitors. *Bioorg. Chem.* **2020**, 98, 103711.
34. Hasanin, M.; Hashem, A.H.; El-Rashedy, A.A.; Kamel, S. Synthesis of novel heterocyclic compounds based on dialdehyde cellulose: characterization, antimicrobial, antitumor activity, molecular dynamics simulation and target identification. *Cellulose* **2021**, 28, 8355-8374.
35. Machaba, K.E.; Mhlongo, N.N.; Soliman, M.E.S. Induced mutation proves a potential target for TB therapy: A molecular dynamics study on LprG. *Cell Biochem. Biophys*. **2018**, 76, 345-356.
36. Cournia, Z.; Allen, B.; Sherman, W. Relative binding free energy calculations in drug discovery: Recent advances and practical considerations. *J. Chem. Inf. Model.* **2017**, 57, 2911-2937.
37. Skehan, P.; Storeng, R.; Scudiero, D.; Monks, A.; McMahon, J.; Vistica, D.; Warren, J.T.; Bokesch, H.; Kenney, S.; Boyd, M.R. New colorimetric cytotoxicity assay for anticancer-drug screening. *JNCI* **1990**, 82, 1107-1112.
38. Podust, L.M.; Poulos, T.L.; Waterman, M.R. Crystal structure of cytochrome P450 14α-sterol demethylase (CYP51) from *Mycobacterium tuberculosis* in complex with azole inhibitors. *Proc. Natl. Acad. Sci. USA* **2001**, 98, 3068-3073.
39. Shaikh, Z.; Ashiq, U.; Jamal, R.A.; Gul, S.; Mahroof-Tahir, M.; Sultan, S.; Salar, U.; Khan, K.M. Synthesis, characterization, lipoxygenase, and tyrosinase inhibitory activities of non-cytotoxic titanium(III) and (IV) hydrazide complexes. *Bull. Chem. Soc. Ethiop.* **2023**, 37, 315-333.
40. Li, H.; Robertson, A.D.; Jensen, J.H. Very fast empirical prediction and rationalization of protein pK_a values. *Proteins: Struct. Funct. Bioinform.* **2005**, 61, 704-721.
41. Halford, B. Reflections on CHEMDRAW. *Chem. Eng. News.* **2014**, 92, 26-27.
42. Hospital, A.; Goñi, J.R.; Orozco, M.; Gelpí, J.L. Molecular dynamics simulations: advances and applications. *Adv. Appl. Bioinform. Chem.* **2015**, 8, 37-47.
43. Lee, T.S.; Cerutti, D.S.; Mermelstein, D.; Lin, C.; LeGrand, S.; Giese, T.J.; Roitberg, A.; Case, D.A.; Walker, R.C.; York, D.M. GPU-accelerated molecular dynamics and free energy

methods in Amber18: Performance enhancements and new features. *J. Chem. Inf. Model.* **2018**, 58, 2043-2050.
44. Wang, J.; Wang, W.; Kollman, P.A.; Case, D.A. Automatic atom type and bond type perception in molecular mechanical calculations. *J. Mol. Graph. Model* **2006**, 25, 247-260.
45. Berendsen, H.J.; Postma, J.V.; Van Gunsteren, W.F.; DiNola, A.R.H.J.; Haak, J.R. Molecular dynamics with coupling to an external bath. *J. Chem. Phys.* **1984**, 81, 3684-3690.
46. Roe, D.R.; Cheatham III, T.E. PTRAJ and CPPTRAJ: Software for processing and analysis of molecular dynamics trajectory data. *J. Chem. Theory Comput.* **2013**, 9, 3084-3095.
47. Seifert, E. OriginPro 9.1: Scientific data analysis and graphing software-software review. *J. Chem. Inf. Model.* **2014**, 54, 1552.
48. Rahimzade, S.G.; Akverdieva, G.A. Structural analysis of Val-Trp dipeptide: Molecular mechanics and DFT calculations. *Bull. Chem. Soc. Ethiop.* **2023**, 37, 757-770.
49. Kollman, P.A.; Massova, I.; Reyes, C.; Kuhn, B.; Huo, S.; Chong, L.; Lee, M.; Lee, T.; Duan, Y.; Wang, W.; Donini, O. Calculating structures and free energies of complex molecules: Combining molecular mechanics and continuum models. *Acc. Chem. Res.* **2000**, 33, 889-897.